ACS APPLIED MATERIALS & INTERFACES

Research Article

www.acsami.org

Functional Mesoporous Silica Nanoparticles for the Selective Sequestration of Free Fatty Acids from Microalgal Oil

Justin S. Valenstein, Kapil Kandel, Forrest Melcher, Igor I. Slowing, Victor S.-Y. Lin,[†] and Brian G. Trewyn*

Department of Chemistry and U.S. Department of Energy-Ames Laboratory, Iowa State University, Ames, Iowa 50011, United States

ABSTRACT: A series of 2d-hexagonally packed mesoporous silica nanoparticle material with 10 nm pore diameter (MSN-10) covalently functionalized with organic surface modifiers have been synthesized via a post-synthesis grafting method. The material structure has been characterized by powder X-ray diffraction, electron microscopy, and nitrogen sorption analyses, and the free fatty acid (FFA) sequestration capacity and selectivity was investigated and quantified by thermogravimetric and GC/MS analysis. We discovered that aminopropyl functionalized 10 nm pore mesoporous silica nanoparticle material (AP-MSN-10) sequestered all available FFAs and left nearly all other molecules in solution from a simulated microalgal extract containing FFAs, sterols, terpenes, and triacylglycerides. We also demonstrated selective FFA sequestration from commercially available microalgal oil.

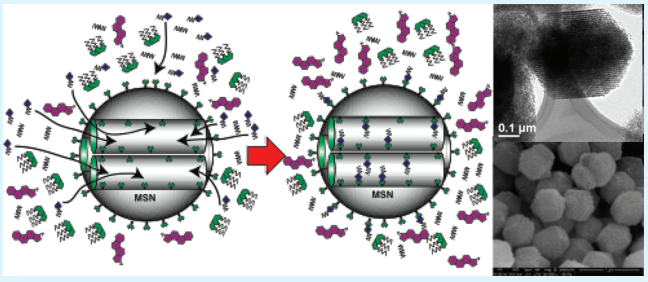

KEYWORDS: *mesoporous silica, free fatty acids, selective sequestration, microalgal oil*

INTRODUCTION

The U.S. and the European Union produce nearly 1.5 billion liters of biodiesel annually.[1] The high cost of biodiesel can be greatly attributed to the high costs of the oil feedstock and are slowing the global commercialization. One solution is to use waste oils[2,3] and nonfood sources[4] as feedstocks. Algae present themselves as a potential feedstock source because many species grow in oceanwater or wastewater and produce more energy than other biofuel crops.[5] The large-scale production of biodiesel was recently demonstrated by Li and co-workers when they published the requirements to successfully grow algae to a density of 14.2 g L^{-1} in an 11 000 L bioreactor with a lipid content of 44.3% dry weight and converted the oil to fatty acid methyl esters (FAMEs or biodiesel) through transesterification using immobilized lipase.[6]

Because algae are known to produce a wide variety of high-value and value-added hydrocarbons and lipids,[7,8] it is necessary to develop technology to separate the algae-produced molecules to optimize the economics of converting algae oil to energy. An example of a high-value hydrocarbon found in algae is free fatty acids (FFAs), where some have considerable value to the pharmaceutical, neutraceutical, and cosmetic industries, particularly the omega-3 and other polyunsaturated FFAs. Another reason to selectively sequester FFAs from feedstocks is the negative effects they have on the conversion of oils to biodiesel. Biodiesel is currently produced from very low FFA percentage (<1%) crop oils by the conversion of triacylglycerides (TAGs) through a base-catalyzed transesterification. When the concentration of acid in the feedstock is too high, as they are often found in algal oil, the basic catalyst is neutralized and additional catalyst is required to maintain the reaction kinetics.

Current separation and purification methods for organic acids are challenging and energy intensive, with extraction and distillation the most common techniques, either using organic solvents or supercritical fluids.[9−11]

The discovery and development of surfactant micelle-templated mesoporous silica nanoparticle (MSN) materials with high surface area and pore volume have advanced the utilization of these materials for applications in catalysis,[12,13] sensors,[14] delivery vessels,[15−20] and adsorbents.[21] One unique property of MSN is the ease and control at which the surfaces can be functionalized with organic moieties. The performance of the MSN in these sequestration applications is strongly dependent upon the surface functionalization; the interaction between the MSN and specific molecules will vary depending on the nature of the surface chemistry.

Herein, we report the synthesis of a series of mesoporous silica nanoparticles of similar pore diameters with various surface functional groups as sequestration nanomaterials for FFAs. The structure of the resulting materials were investigated via standard material characterization methods including powder X-ray diffraction (XRD), transmission electron microscopy (TEM), scanning electron microscopy (SEM), and nitrogen sorption analysis. The sequestration capacity and FFA selectivity was demonstrated in a simulated feedstock oil with the optimized MSN material to determine the feasibility of using this material

Received: November 23, 2011
Accepted: January 11, 2012
Published: January 11, 2012

   dx.doi.org/10.1021/am201647t | *ACS Appl. Mater. Interfaces* 2012, 4, 1003−1009

for the isolation and purification of FFA from microalgal feedstocks. We discovered that aminopropyl functionalized MSN, with 10 nm pore diameter (AP-MSN-10), selectively sequestered FFAs. The high affinity of amines as adsorbents for organic acids[21] coupled with the high surface area and uniform pore structure of the mesoporous material[22] makes the amine-functionalized mesoporous material an ideal candidate for FFA adsorption. Finally, we demonstrated the selective FFA sequestration ability of AP-MSN-10 from a crude, commercially produced algae oil feedstock.

EXPERIMENTAL SECTION

MSN-10.[23] The nonionic surfactant Pluronic P104 (7.0 g) was added to 1.6 M HCl (273.0 g). After stirring for 1 h at 55 °C, tetramethylorthosilicate (TMOS, 10.64 g) was added and stirred for an additional 24 h. The resulting mixture was further posthydrothermally treated for 24 h at 150 °C in a high-pressure reactor. Upon cooling to room temperature, the white solid was collected by filtration, washed with copious amounts of methanol and dried in air. To remove the surfactant P104 by calcination, the MSN material was heated at a ramp rate of 1.5 °C min^{-1} and maintained at 550 °C for 6 h.

x-MSN-10. Functionalized MSN-10 will be denoted as x-MSN-10, where x represents the organoalkoxysilane. Organoalkoxysilane (3 mmol) was added to a toluene suspension (100 mL) of MSN-10 (1.0 g). The suspension was refluxed for 20 h under nitrogen. The resulting material was filtered, washed with toluene and methanol, and dried under vacuum overnight. The silanes used to functionalize the MSN-10 were 3-aminopropyltrimethoxysilane (AP), benzyltrimethoxysilane (Bz), hexadecyltrimethoxysilane (Hex), 1-propyl-3-methyl imidazolium bromide trimethoxysilane (PMIm), and 3-mercaptopropyltrimethoxysilane (MP).

AP-Silica Gel. 3-aminopropyltrimethoxysilane (3 mmol) was added to a toluene suspension (100 mL) of silica gel (1.0 g). The suspension was refluxed for 20 h under nitrogen. The resulting material was filtered, washed with toluene and methanol, and dried under a vacuum overnight.

Material Characterization. Powder X-ray diffraction experiments were performed on a Rigaku Ultima IV diffractometer using a Cu Kα radiation source. Low angle diffraction with a 2θ range of 0.8−6° was used to investigate the long-range order of the porous materials. TEM studies were done by placing a small aliquot of an aqueous suspension on a lacey carbon film coated 400 mesh copper grid and drying it in air. The TEM images were obtained on a Tecnai F^2 microscope. Particle morphology was determined by SEM using a Hitachi S4700 FE-SEM system with 10 kV accelerating voltage. The surface area and average pore diameter were measured using N_2 adsorption/desorption measurements in a Micromeritics ASAP 2020 BET surface analyzer system. The data were evaluated using Brunauer−Emmett−Teller (BET) and Barrett−Joyner−Halenda (BJH) methods to calculate surface area and pore distributions, respectively. Samples were prepared by degassing at 100 °C overnight before analysis. Surface functional group loadings were determined by TGA. For TGA, 10 mg samples were heated from 25 to 650 °C in air at a heating rate of 2 °C min^{-1} using a TA Instruments model 2950 thermogravimetric analyzer. The subsequent data were analyzed by Universal Analysis 2000 software. Zeta-potential measurements were carried out by sonicating 5 mg of sample in 5 mL of PBS for 30 min. The samples were then analyzed on a Malvern Instruments Zetasizer. All adsorption studies were done using GC-MS analysis. Samples were dissolved in hexanes and analyzed using an Agilent Technologies 7890A gas chromatograph equipped with a HP-5 ms column in-line with a 5975C mass detector.

Adsorption Experiments. Adsorption experiments were conducted using 16 × 125 mm culture tubes. The adsorbent MSN material (25 mg) was suspended in a 10 mL hexane solution containing either a single component or a mixture of components that make up the microalgal simulated solution for 6 h. The adsorbate was separated from the solution using centrifugation and the supernatant was analyzed by GC-MS.

Microalgal Simulated Solution. A mixture of naturally occurring microalgal products[7,8] was prepared to investigate the adsorption selectivity. Palmitic acid (57 μM), glyceryl tristearate (400 μM), squalene (114 μM), and ergosterol (57 μM) were all dissolved in a single solution of hexanes.

Microalgal Oil Adsorption. Crude microalgal oil obtained from Solix Biofuels, Inc., was used for testing the sequestration abilities of amine functionalized MSN-10 and amine functionalized silica gel. Silica material (100 or 300 mg) was added to 200 mg of microalgal oil in 10 mL hexanes and mixed for 6 h.

Methyl Esterification of Free Fatty Acids. Esterification of the MSN adsorbed FFAs was necessary for quantitative analysis via GC/MS. The hexanes were removed under reduced pressure. To the resulting residue was added 0.01 M HCl in methanol (4 mL) and nonadecanoic acid, as an internal standard, and the mixture was stirred for 1 h at 80 °C. After the mixture was cooled to room temperature, 1% NaCl (1 mL) was added to the reaction mixture to increase the recovery of fatty acid methyl esters (FAMEs) from the reaction mixture by solvent extraction. The FAMEs were extracted with subsequent portions of hexane (3 × 3 mL). The combined portions were diluted to a final volume of 10 mL with hexane and transferred to a GC vial for analysis by GC/MS.

Silylation of Sterols.[24] Derivatization of sterols is necessary for quantification via GC/MS. The hexanes were removed under reduced pressure. Hexanes (2 mL) and 1 mL Sylon (BSTFA (N,O-bis(trimethylsilyl)trifluoroacetamide) and TMCS (trimethylchlorosilane), 99:1) were added to the residue and heated to 70 °C for 1 h while stirring. The products were diluted to a final volume of 10 mL with hexane and transferred to GC vials for analysis by GC/MS.

Transesterification of Triacylglycerides. Transesterification of triacylglycerides are necessary for quantification via GC/MS. The hexanes were removed under reduced pressure and the resulting residue was dissolved in 4 mL of 0.04 M methanolic NaOH. The mixture was heated to 75 °C for 1 h while stirring. After the mixture was cooled to room temperature, 1% NaCl (1 mL) was added to the reaction mixture. The FAMEs were extracted with subsequent portions of hexane (3 × 3 mL). The combined portions were diluted to a final volume of 10 mL with hexane and transferred to a GC vial for analysis by GC/MS.

Titration of Free Fatty Acids. The free fatty acids remaining in solution from the algal oil are quantified by titration with KOH. The hexanes were removed under reduced pressure and resulting residue was dissolved in 125 mL isopropyl alcohol that was previously neutralized with KOH. A few drops of phenolphthalein solution were added to the alcohol mixture and titrated with 0.05 M KOH until a color change was observed. The titration of FFAs was repeated to produce a triplicate of experiments.

RESULTS AND DISCUSSION

Screening of MSN Pore Size Dependence on FFA Sequestration. Initially, two mesoporous silica nanoparticle (MSN) materials with different pore sizes were synthesized and tested to determine the FFA sequestration dependence on pore diameter. Mesoporous silica nanoparticle material with a pore diameter of 2.5 nm (MSN-2.5) were synthesized following a previously reported method[25] and MSN with 10 nm pores (MSN-10) were synthesized by modifying Linton's procedure.[26] The two MSN materials were individually mixed with a hexane solution of FFAs for 6 h and the FFAs remaining in the supernatant were analyzed by GC-MS. The FFA sequestration capacity of MSN-2.5 and MSN-10 were 0.40 and 0.65 mmol FFA g^{-1}, respectively. Because MSN-10 was shown to sequester 63% more FFAs, it was chosen as the base material for continued studies.

Characterization of the x-MSN-10s. The organoalkoxysilanes that were utilized to functionalize the MSN by postsynthetic

Table 1. Structure Properties of MSN-10 and x-MSN-10

sample	d_{100} (Å)	a_0 (Å)	$W_{BJH}{}^a$ (Å)	$S_{BET}{}^a$ (m^2 g^{-1})	PV^a (cm^3 g^{-1})	loading^b (mmol g^{-1})	zeta potential (mV)
MSN-10	100.38	115.91	104.7	375	1.02		−28.1
AP-MSN-10	92.02	106.25	100.7	290	0.78	1.54	+19.3
Bz-MSN-10	90.09	104.03	101.0	266	0.72	1.25	−19.8
Hex-MSN-10	86.63	100.03	98.3	265	0.94	0.68	−21.7
PMIm-MSN-10	90.14	104.08	101.2	281	0.76	1.34	+28.7
MP-MSN-10	91.85	106.06	100.3	233	0.86	1.20	−22.4

$^a W_{BJH}$ represents the pore diameter; S_{BET} represents the surface area; PV represents the pore volume ^{b}Loading represents the amount of functional group grafted on to the materials

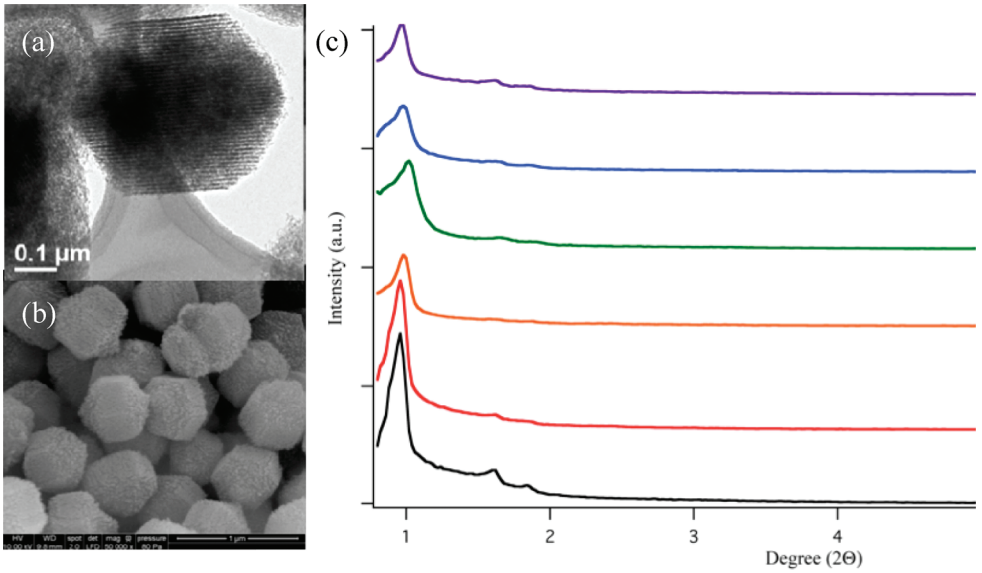

Figure 1. (a) Transmission electron micrograph, (b) scanning electron micrograph, and (c) XRD spectra of the surfactant removed unfunctionalized MSN-10 (black), AP-MSN-10 (red), Bz-MSN-10 (orange), Hex-MSN-10 (green), PMIm-MSN-10 (blue), and MP-MSN-10 (purple).

grafting were 3-aminopropyltrimethoxysilane (AP), benzyltrimethoxysilane (Bz), hexadecyltrimethoxysilane (Hex), 1-propyl-3-methyl imidazolium bromide trimethoxysilane (PMIm), and 3-mercaptopropyltrimethoxysilane (MP). To functionalize the MSN-10, we added 3 mmol g^{-1} of each organoalkoxysilane to a refluxing toluene suspension of the mesoporous material. The amount of each functional group loaded on the surface of MSN-10 can be found in Table 1 as determined by TGA analysis. The X-ray diffraction patterns of x-MSN-10 are shown in Figure 1c. The observed diffraction patterns with intense (d_{100}) peaks are characteristic of highly ordered two-dimensional (2D) hexagonal mesostructures with uniform channels.[27] To directly visualize the pore structure, we analyzed the x-MSN-10 materials by transmission electron microscopy (TEM). As shown in Figure 1a, the parallel stripes indicate that the postsynthetic grafting did not destroy the cylindrical mesoporous channels,[17] which is consistent with the XRD measurements. The scanning electron micrograph (SEM) in Figure 1b shows the particles have a spherical structure and not a flat, disk-like shape.[26] The maintenance of the pore structure is also confirmed by nitrogen sorption analysis using BET and BJH calculations, see Figure 2 for isotherms. A small decrease in the pore diameter of appoximately 0.5 nm is observed after functionalization, along with a drop in surface area (375 m^2 g^{-1} to 290 m^2 g^{-1}). Thermogravimetric analysis (TGA)

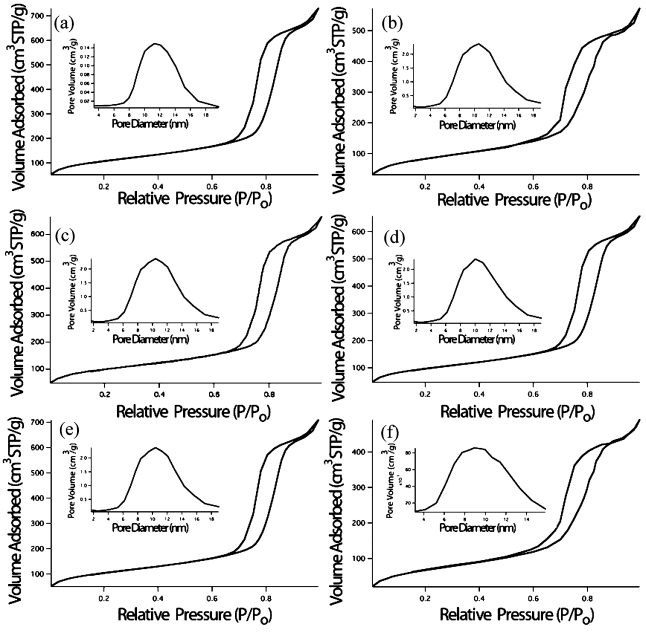

Figure 2. BET isotherms and BJH pore size distributions (insets) of MSN-10 (a), AP-MSN-10 (b), Bz-MSN-10 (c), Hex-MSN-10 (d), PMIm-MSN-10 (e), and MP-MSN-10 (f).

of x-MSN-10s was utilized to determine the loading amounts of each organoalkoxysilane. A summary of all of the characterization measurements can be found in Table 1.

Selection of the Optimal Functional Group for FFA Sequestration. To determine the organic functional group that optimized the effectiveness of our adsorbent material, the resulting x-MSN-10 materials were mixed with a hexane solution of FFAs and the FFAs remaining in solution were analyzed. The results varied but AP-MSN-10 sequestered 98% of available FFA (0.98 mmol FFA g MSN^{-1} from a 1.0 mM FFA solution), followed by Bz-MSN-10, which sequestered 0.50 mmol FFA g MSN^{-1}, see Table 2 for a complete list of the

Table 2. Adsorption Dependence of FFAs on MSN Surface Grafted Functional Group

functional group (x-trialkoxysilane)	amount adsorbed (mmol FFA g MSN^{-1})	amount adsorbed (mmol FFA m^{-2})
none	0.65	0.0017
3-aminopropyl	0.98	0.0034
benzyl	0.50	0.0019
hexadecyl	0.30	0.0011
1-propyl-3-methyl imidazolium bromide	0.40	0.0014
3-mercaptopropyl	0.25	0.0011

sequestration results by mass and surface area of MSN. The high sequestration capacity per unit of surface area of the AP-MSN-10 lends itself to be used as an adsorbent for FFAs.

Adsorption Isotherms. The kinetics of palmitic acid adsorption on AP-MSN-10 was measured (Figure 3) to

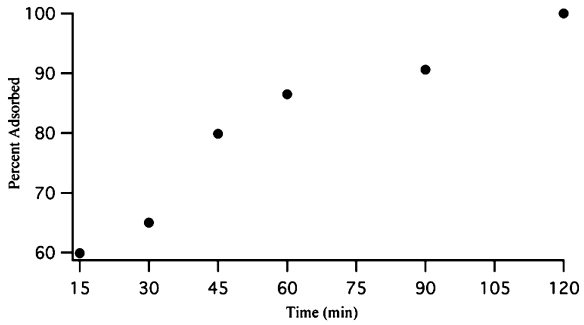

Figure 3. Amount of palmitic acid adsorbed on AP-MSN-10 as a function of contact time (initial [palmitic acid] = 2.1 mM).

determine the time required for equilibrium to be reached between the adsorbent and adsorbate. The amount of acid adsorbed on the AP-MSN-10 reached 100% at 120 min. The adsorbent capacities of the sequestration materials were determined by treating unfunctionalized MSN-10 and AP-MSN-10 materials with different analytes in varying concentrations that are commonly found in microalgal solutions. The components of the simulated microalgal solution were palmitic acid (FFA), glyceryl tristearate (triacylglyceride), squalene (terpene), and ergosterol (sterol). Data found in Table 3 and the adsorption isotherms indicate AP-MSN-10 has a higher adsorption capacity for FFAs than unfunctionalized MSN-10. Interestingly, an adsorption capacity of 1.50 mmol g^{-1} is equal

Table 3. Q_{max} Values (mmol g^{-1}) for Adsorbates on MSN-10 and AP-MSN-10

	MSN-10	AP-MSN-10
palmitic acid	0.81	1.50
glyceryl tristearate	0.44	0.22
ergosterol	0.48	0.18
squalene	0.0089	0.0063

to the number of surface amine moieties on the surface of AP-MSN-10 (1.53 mmol g MSN^{-1}) as determined by TGA, indicating a 1:1 complexation between the surface amines and free fatty acids and monolayer coverage of the surface. All of the adsorption isotherms that were measured were fitted to the Langmuir equation

$$Q = \frac{k_1 C}{k_2 + C}$$

where Q (mmol g^{-1}) is the amount of adsorbate adsorbed per gram of adsorbent, C is the adsorbate concentration, and k_1 and k_2 are Langmuir adsorption equilibrium constants. The data was fitted to the equation with the coefficient of determination values exceeding 0.95, indicating a statistical goodness of fit. The adsorption isotherms and Langmuir adsorption model curve fits are shown in Figures 4 and 5. In addition to improved FFA adsorption over unfunctionalized MSN-10, AP-MSN-10 had a significantly higher adsorption capacity for FFAs compared to the other classes of adsorbates. The nonfunctionalized MSN-10 reached an adsorption capacity of 0.81 mmol g^{-1} for palmitic acid compared to the maximum adsorption capacity of 1.50 mmol g^{-1} for palmitic acid on the AP-MSN-10. In addition, the adsorption capacity of 1.50 mmol g^{-1} is much higher than previous reports for porous silica materials ranging from 0.18 to 0.6 mmol g^{-1}.[28−30]

Selectivity of AP-MSN-10. To demonstrate the selectivity of AP-MSN-10 for FFAs, 25 mg of AP-MSN-10 was mixed with 10 mL of a simulated solution closely resembling microalgal oil containing a mixture of palmitic acid (57 μM), glyceryl tristearate (400 μM), squalene (114 μM), and ergosterol (57 μM). After removal of the AP-MSN-10 from the solution, the hydrocarbons remaining in solution were quantified. The results of the selectivity experiments are listed in Table 4. AP-MSN-10 exhibited a dramatic preference for adsorbing palmitic acid over all the other substances, while MSN-10 adsorbed all substances equally except for squalene. This phenomenon can be explained by the surface amines of AP-MSN-10 acting as specific binding sites for FFAs. According to Bruckenstein and Untereker, an uncharged complex will form in hexane resulting from the exchange of the acidic proton from the FFA to the primary amine.[31] This phenomenon is used to explain the high selectivity of AP-MSN-10 toward FFAs. The other three classes of adsorbates do not contain an acidic proton or in the case of ergosterol, the pK_a is too high to exchange with the surface amine. Although unfunctionalized MSN-10 did not demonstrate any selectivity, the incorporation of the amine group greatly shifted the selectivity of the mesoporous material toward free fatty acids.

Recyclability of AP-MSN-10. The recyclability of AP-MSN-10 was tested by repeated experiments of palmitic acid

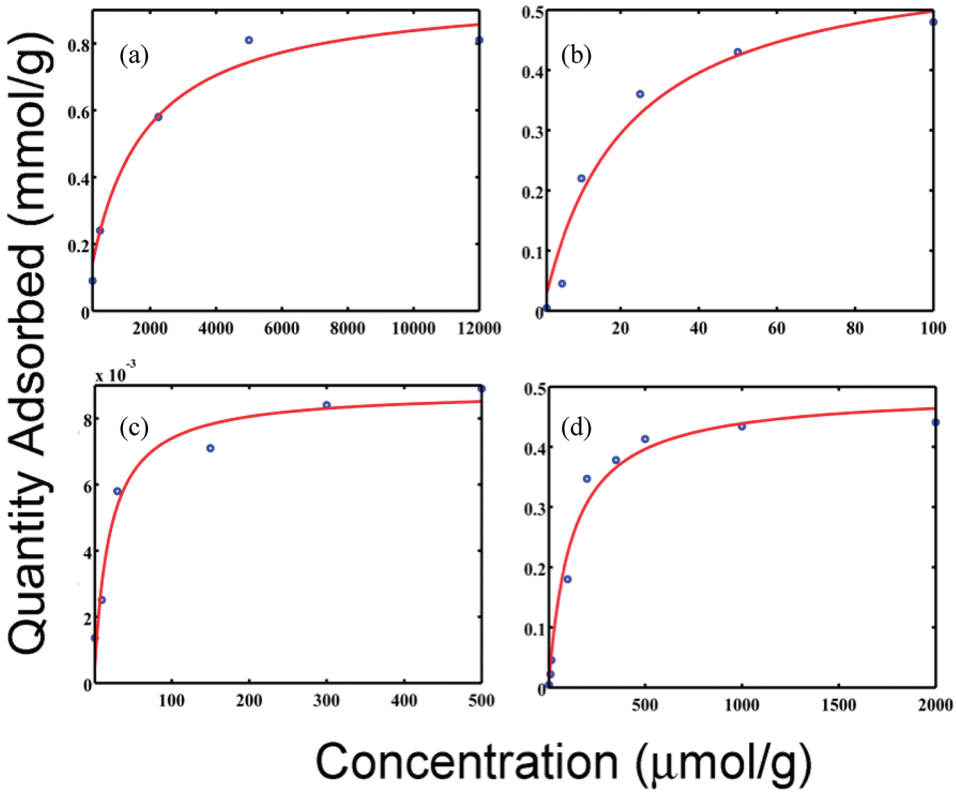

Figure 4. Adsorption isotherms of (a) palmitic acid, (b) ergosterol, (c) squalene, and (d) glyceryl tristearate adsorbed on MSN-10.

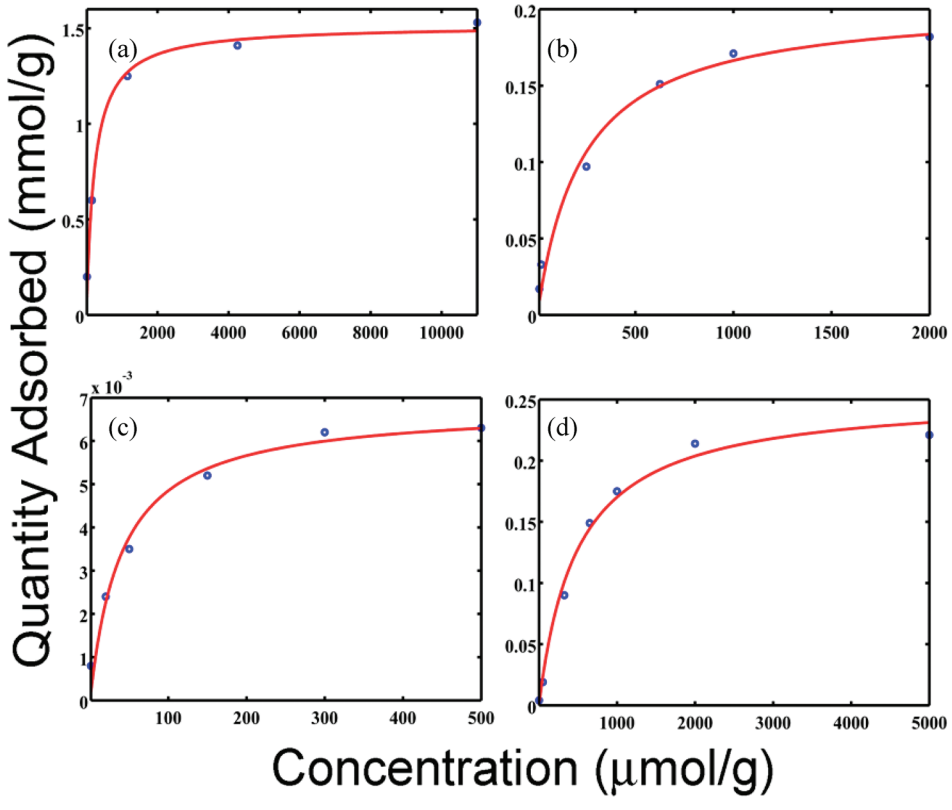

Figure 5. Adsorption isotherms of (a) palmitic acid, (b) ergosterol, (c) squalene, and (d) glyceryl tristearate adsorbed on AP-MSN-10.

adsorption. The AP-MSN-10 with adsorbed palmitic acid was added to the esterification reaction mixture to transform the acids to the methyl esters. By reacting the acidic proton involved in the complexation responsible for the acid selectivity,

dx.doi.org/10.1021/am201647t | ACS Appl. Mater. Interfaces 2012, 4, 1003–1009

Table 4. Adsorption Values (mmol g^{-1}) from Simulated Microalgal Oil for MSN-10 and AP-MSN-10

	MSN-10	MSN-10 % sequestered	AP-MSN-10	AP-MSN-10 % sequestered
palmitic acid	0.0228	100	0.0228	100
glyceryl tristearate	0.150	93.8	0.012	7.5
ergosterol	0.0228	100	0.0039	17.1
squalene	0.0082	17.9	0.0048	10.5

we can desorb the sequestered molecules from the surface of the AP-MSN-10. After the first cycle of adsorption, we are able to recover 92% of the adsorbed palmitic acid; however, the adsorption efficiency of the second and third cycles dropped to 73% and 59% of the first cycle, respectively. The decrease in adsorption efficiency is likely due to the remaining acid still adsorbed to the silica surface after desorption is attempted and the harsh conditions of the acid-catalyzed esterification deteriating the silica material. Active research is currently underway to identify less harsh, more efficient methods to recycle the sequestration MSN material.

Adsorption of FFAs by AP-MSN-10 from Commercial Microalgal Oil. To demonstrate the selective adsorption ability of the AP-MSN-10 with commercially available microalgal oil, 100 mg AP-MSN-10 and 300 mg AP-silica gel, as a control, were mixed with microalgal oil obtained from Solix, Inc. (Fort Collins, CO). Once the materials were separated from the oil, the supernatant was analyzed for remaining FFA content. Using varying amounts of material, AP-MSN-10 adsorbed 1.50 mmol FFA g^{-1} compared to the 0.38 mmol FFA g^{-1} for the AP-silica gel. The increase in surface area and pore volume by the incorporation of mesopores into the structure of the silica adsorbent plays a vital role in increasing the adsorption capacity. Both adsorption quantities closely match the amount of amine groups grafted on the surface of each material. The AP-MSN-10 is able to maintain the adsorption capabilities in a complex mixture applicable to current processes.

Further experiments were conducted using AP-MSN-10 for the adsorption of FFAs from commercial microalgal oil. By using the calculated value for amine moieties on the surface of AP-MSN-10, we determined the amount of material necessary to introduce a 1:1 ratio of amine groups to FFA in the microalgal oil. A 100 mg aliquot of microalgal oil was dissolved in hexanes and mixed with 25 mg of AP-MSN-10 for 2 h. After separating the silica materials from the supernatant, the supernatant was added to a second vial for a second adsorption cycle. The remaining FFAs were analyzed by titration. The FFA content of the microalgal oil was reduced from 11.5% to 3.2% after the first cycle and 0.70% after the second cycle, calculated by KOH titration. Reducing the FFA content to less than 1% will increase the feasibility of using current industrial transesterification catalysts for microalgal biodiesel.

CONCLUSIONS

In summary, the successful synthesis and characterization of aminopropyl-functionalized 10 nm pore mesoporous silica nanoparticle material has been demonstrated. We showed that functionalizing MSN-10 was necessary to optimize the sequestration capacity and selectivity for FFAs (see Scheme 1). The addition of the primary amine group to the surface of MSN-10 increased the adsorption capacity from 0.8 to 1.50 mmol FFA g^{-1} and improved the selectivity from 11 to 53 mol % uptake by utilizing proton exchange to create specific binding sites for FFAs. We have also demonstrated the ability to reduce the FFA content of microalgal oil to less than 1% using AP-MSN-10, which makes it more favorable to be used as a biodiesel source. We are currently establishing a series of mesoporous nanomaterials that are specific for different biomolecules produced by microorganisms.

Scheme 1. Schematic Illustrating the Selective Uptake and Sequestration of the Free Fatty Acids from a Solution of Lipids and Hydrocarbons Found in Microalgal Oil

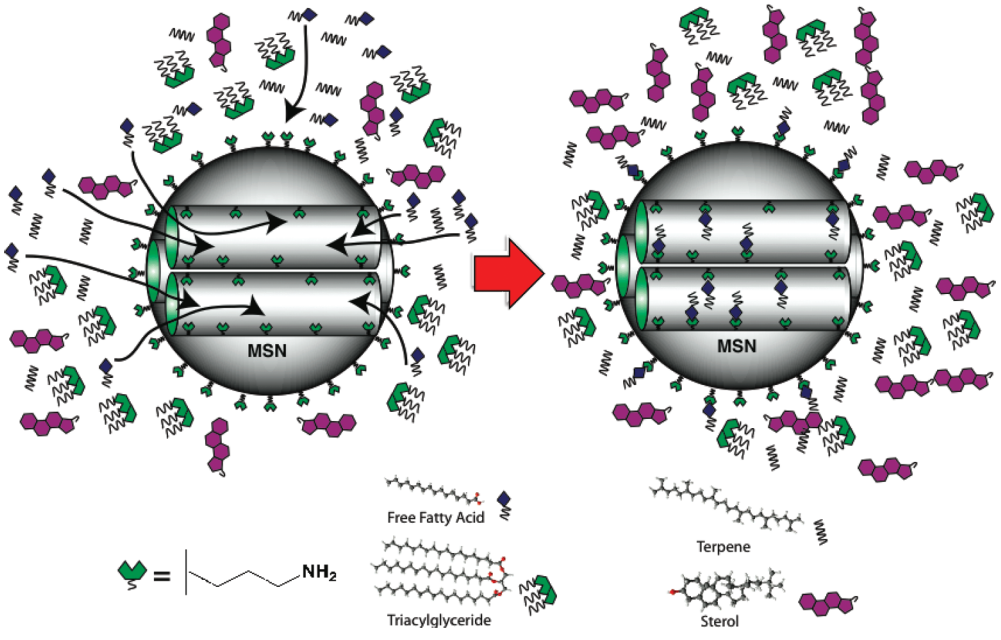

dx.doi.org/10.1021/am201647t | ACS Appl. Mater. Interfaces 2012, 4, 1003–1009

AUTHOR INFORMATION

Corresponding Author

*E-mail: bgtrewyn@iastate.edu.

Notes

†Deceased May 4, 2010

ACKNOWLEDGMENTS

B.G.T., I.I.S., and J.S.V. thank the U.S. Department of Energy, Office of Energy Efficiency and Renewable Energy (Grant DE-FG26-0NT08854), for financial support. B.G.T., K.K., and F.M. also acknowledge funding of this work by the U.S. Department of Energy under Contract DE-EE0003046 awarded to the National Alliance for Advanced Biofuels and Bioproducts.

REFERENCES

(1) Gerpan, J. V. *Fuel Process. Technol.* **2005**, *86* (10), 10.
(2) Yoshimura, T. *Petrotech (Tokyo)* **1998**, *21* (10), 967−972.
(3) Zhang, Y.; Dube, M. A.; McLean, D. D.; Kates, M. *Bioresour. Technol.* **2003**, *90* (3), 229−240.
(4) Cheng, Y.; Lu, Y.; Gao, C.; Wu, Q. *Energy Fuels* **2009**, *23* (8), 4166−4173.
(5) Chisti, Y. *Biotechnol. Adv.* **2007**, *25* (3), 294−306.
(6) Li, X.; Xu, H.; Wu, Q. *Biotechnol. Bioeng.* **2007**, *98* (4), 764−771.
(7) Metzger, P.; Largeau, C. *Appl. Microbiol. Biotechnol.* **2005**, *66* (5), 486−496.
(8) Zhila, N. O.; Kalacheva, G. S.; Volova, T. G. *Russ. J. Plant Physiol.* **2005**, *52* (3), 311−319.
(9) Angenent, L. T.; Karim, K.; Al-Dahhan, M. H.; Wrenn, B. A.; Domiguez-Espinosa, R. *Trends Biotechnol.* **2004**, *22* (9), 477−485.
(10) Bungay, H. R. *Trends Biotechnol.* **2004**, *22* (2), 67−71.
(11) Wu, Z.; Yang, S.-T. *Biotechnol. Bioeng.* **2003**, *82* (1), 93−102.
(12) Chen, H.-T.; Huh, S.; Wiench, J. W.; Pruski, M.; Lin, V. S. Y. *J. Am. Chem. Soc.* **2005**, *127* (38), 13305−13311.
(13) Nieweg, J. A.; Lemma, K.; Trewyn, B. G.; Lin, V. S. Y.; Bakac, A. *Inorg. Chem.* **2005**, *44* (16), 5641−5648.
(14) Zhao, Y.; Trewyn, B. G.; Slowing, I. I.; Lin, V. S. Y. *J. Am. Chem. Soc.* **2009**, *131* (24), 8398−8400.
(15) Giri, S.; Trewyn, B. G.; Stellmaker, M. P.; Lin, V. S. Y. *Angew. Chem., Int. Ed.* **2005**, *44* (32), 5038−5044.
(16) Lai, C.-Y.; Trewyn, B. G.; Jeftinija, D. M.; Jeftinija, K.; Xu, S.; Jeftinija, S.; Lin, V. S. Y. *J. Am. Chem. Soc.* **2003**, *125* (15), 4451−4459.
(17) Radu, D. R.; Lai, C.-Y.; Jeftinija, K.; Rowe, E. W.; Jeftinija, S.; Lin, V. S. Y. *J. Am. Chem. Soc.* **2004**, *126* (41), 13216−13217.
(18) Slowing, I. I.; Trewyn, B. G.; Lin, V. S. Y. *J. Am. Chem. Soc.* **2007**, *129* (28), 8845−8849.
(19) Torney, F.; Trewyn Brian, G.; Lin Victor, S. Y.; Wang, K. *Nat. Nanotechnol.* **2007**, *2* (5), 295−300.
(20) Trewyn, B. G.; Whitman, C. M.; Lin, V. S. Y. *Nano Lett.* **2004**, *4* (11), 2139−2143.
(21) Jun, Y.-S.; Huh, Y. S.; Park, H. S.; Thomas, A.; Jeon, S. J.; Lee, E. Z.; Won, H. J.; Hong, W. H.; Lee, S. Y.; Hong, Y. K. *J. Phys. Chem. C* **2007**, *111* (35), 13076−13086.
(22) Lin, V. S. Y.; Lai, C.-Y.; Huang, J.; Song, S.-A.; Xu, S. *J. Am. Chem. Soc.* **2001**, *123* (46), 11510−11511.
(23) Kim, T.-W.; Slowing, I. I.; Chung, P.-W.; Lin, V. S.-Y. *ACS Nano* **2011**, *5* (1), 360−366.
(24) Blau, K., Halket, J. *Handbook of Derivatives for Chromatography*, 2nd ed; John Wiley & Sons: New York, 1993.
(25) Huh, S.; Wiench, J. W.; Yoo, J.-C.; Pruski, M.; Lin, V. S. Y. *Chem. Mater.* **2003**, *15* (22), 4247−4256.
(26) Linton, P.; Alfredsson, V. *Chem. Mater.* **2008**, *20* (9), 2878−2880.
(27) Zhao, D.; Huo, Q.; Feng, J.; Chmelka, B. F.; Stucky, G. D. *J. Am. Chem. Soc.* **1998**, *120* (24), 6024−6036.
(28) Gao, Q.; Xu, W.; Xu, Y.; Wu, D.; Sun, Y.; Deng, F.; Shen, W. *J. Phys. Chem. B* **2008**, *112* (7), 2261−2267.
(29) O'Connor, A. J.; Hokura, A.; Kisler, J. M.; Shimazu, S.; Stevens, G. W.; Komatsu, Y. *Sep. Purif. Technol.* **2006**, *48* (2), 197−201.
(30) Topallar, H.; Bayrak, Y. *Turk. J. Chem.* **1999**, *23* (2), 193−198.
(31) Bruckenstein, S.; Untereker, D. F. *J. Am. Chem. Soc.* **1969**, *91* (21), 5741−5.